Vietnam Journal of Catalysis and Adsorption
Tạp chí xúc tác và hấp phụ Việt Nam

http://chemeng.hust.edu.vn/jca/

Size-controlled synthesis of alginate-stabilized Cu_2O@Cu nanoparticles: effect of stabilizer agent concentration on particle size

Le Nghiem Anh Tuan[1,2], Doan Thi Bich Ngoc[2], Tran Phuoc Tho[2], Nguyen Hong Nhung[3], Bui Duy Du[1,2*]

[1] *Institute of Applied Materials Science, Vietnam Academy of Science and Technology, Ho Chi Minh City, VIETNAM*
[2] *Graduate University of Science and Technology, Vietnam Academy of Science and Technology, Hanoi, VIETNAM*
[3] *PetroVietNam Fertilizer and Chemicals Corporation, Ho Chi Minh City, VIETNAM*
**Email: vina9802@gmail.com*

ARTICLE INFO

Received: 14/02/2021
Accepted: 19/7/2021
Published: 15/10/2021

Keywords:

Alginate-stabilized, Cu_2O@Cu nanoparticles, alginate concentration

ABSTRACT

Alginate-stabilized Cu_2O@Cu nanoparticles were fabricated by chemical reduction method using nature polymer alginate as a stabilizing agent. Transmission electron microscopy (TEM), X-ray powder diffraction (XRD), infrared (FT-IR) spectrum, and UV-Vis analysis were used to investigate the morphology, size, structure, and stability of the nanoparticles synthesized. The results suggested that concentration of alginate has an effect on particle size of Cu_2O@Cu. The particle size of Cu_2O@Cu decreased when the alginate concentration increased. The 5% alginate-stabilized Cu_2O@Cu nanoparticles have small sizes (5.5±1.6 nm). The first, the as-preprated products formed Cu_2O@Cu_2O core-shell nanoparticles structure and final, it would be converted to Cu_2O@Cu core-shell nanoparticles structure.

Introduction

In recent efforts, metallic and metallic oxide nanoparticles have emerged as significant and novel antimicrobial, antifungal agents [1,2-5]. Owing to their nano-dimensions (1-100 nm range), copper oxide nanoparticles exhibit fascinating as well as high anti-microorganism compared to their bulk counterparts [3,4]. Among various practical approaches to preparing Cu_2O-Cu nanoparticles, the chemical reduction approach is considered a straightforward, affordable, and scalable technique [6]. Although the preparation of Cu_2O-Cu nanoparticles has advanced significantly, this technique only works at low copper ion concentrations (< 1,000 mg/L). Due to this reason, it hinders large-scale production [2,3,7]. The main challenge of preparation of Cu-based nanoparticles by the reduction approach is their instability due to aggregation. It is well-known that due to high surface energy, the nanoparticles tend to be aggregated strongly, hence the performance of nanomaterials in particular applications will be affected. To overcome such aggregation, surfactants are often used to improve the colloidal stability of nanoparticles. Among various surfactants, thanks to the strong adhesivity to the metal surface, alginate, a biocompatible, biodegradable, and natural nontoxic polysaccharide, is one of the best candidates for preparation of Cu_2O-Cu nanoparticles [8].

Currently, plant diseases are controlled with the heavy dependence of using rather toxic antibacterial chemicals [9]. The use of chemical bactericides is currently recognized as a danger to human health and the ecosystem, leading to the need of promoting

https://doi.org/10.51316/jca.2021.098

substitutions to mitigate the damage of plant diseases. Recent studies have shown that metal nanoparticles can evolve to become key factors in coping with plant diseases and promoting plant growth [9]. In particular, Cu_2O and Cu nanoparticles showed potential inhibition on various types of bacteria and fungi [3-5]. Huang *et al.* adopted Cu_2O nanoparticles with inhibition of the growth of *Alternaria solani* funguscausing root rot of pepper plant and blight of tomato [10]. The Cu_2O-Cu nanoparticles/alginate expressed high antifungal efficiency (~ 100%) against *Neoscytalidium dimidiatum* causing a brown spot disease on dragon fruit plants, [11] *Xanthomonas oryzae* causing bacterial leaf blight rice, [12] and rice leaf blast disease [13].

Currently, we are interested in alginate-stabilized Cu_2O@Cu nanoparticles prepared by chemical reduction of copper sulfate in alginate solutions using $N_2H_4.H_2O$ as a reducing agent. In the previous study, we reported the effect of copper ion content on particle size of Cu_2O@Cu stabilized by alginate. Herein, we announce the effect of alginate concentration on particle size of alginate-stabilized Cu_2O@Cu nanoparticle and characteristic properties of Cu_2O@Cu nanomaterial by Transmission electron microscopy (TEM), X-ray powder diffraction (XRD), (FT-IR) infrared spectrum, and UV-Vis analysis.

Experimental

Materials

Analytical reagents $CuSO_4.5H_2O$ (99.99%), NH_3 (30%), and $N_2H_4.H_2O$ (80%) were obtained from Merck, Germany. Alginate (Mw ~ 51,200 g/mol) was derived from brown seaweed in Khanh Hoa province, Vietnam.

Preparation of alginate-stabilized Cu_2O@Cu nanoparticles with different alginate concentrations

The preparation of alginate-stabilized Cu_2O@Cu nanoparticles was followed our previous report [11, 12]. 4 g $CuSO_4.5H_2O$ was completely dissolved in 30 mL of water. Afterward, 4 mL NH_3 was added into the $CuSO_4$ solution to produce $[Cu(NH_3)_4]^{2+}$ for preventing gel formation between Cu^{2+} and alginate. Then, the obtained mixture was transferred to sodium alginate solutions, which were prepared by dissolving 8, 10 or 12 g of sodium alginate in 140 mL deionized water for 2 hours. The mixtures were stirred for 10 min before gentle addition of 8 mL hydrazine (N_2H_4, 8% wt.) to reduce Cu^{2+} to Cu^+ and Cu^0. The color of the solution changed from blue to the characteristic reddish-brown color of the alginate-stabilized Cu_2O@Cu nanoparticles. The total volume of the reaction mixtures were adjusted to 200 mL by adding deionized water. The final reaction mixtures have 80 mM Cu content and alginate concentration of 4%, 5% or 6%. The as-preprared products were centrifuged from the solution at 4000 rpm for 15 min and washed with ethanol three times and dried in vacuum drying at 60°C for characterization.

Characterization of alginate-stabilized Cu_2O@Cu nanoparticles

The X-ray diffraction (XRD; D8 Advance Bruker, Germany) measurement was used to study the structure and ingredient of the synthesized materials by applying CuK_α (λ = 1.5405 Å) radiation under a constant current and voltage of 30 mA and 40 kV, respectively, and the diffraction angle (2θ) scan range from 10° to 80°. The infrared spectra were measured by using FT-IR spectrometer (FT-IR 8400S, Shimadzu) over the wavenumber range from 4000 to 400 cm^{-1}. UV-visible absorption spectra 0.2 mM solutions of nanomaterials were recorded with a UV-vis spectrophotometer, Jasco V-630, Japan. Transmission electron microscope measurement (TEM; JEM 1010, JEOL, Tokyo, Japan) was used to study the particle size and morphology of the synthesized materials. Nanoparticle sizes were statistically determined from TEM images by using MS Excel 2010 software. All of the data was expressed as mean ± standard error (SE).

Results and discussion

Characterization of alginate-stabilized Cu_2O@Cu nanoparticles

Figure 1: The color change of solution during the reduction of Cu^{2+} to Cu^+ and Cu^0

Alginate-stabilized Cu_2O@Cu nanoparticles were synthesized from metal precursor copper sulfate pentahydrate ($CuSO_4.5H_2O$) using hydrazine hydrate ($N_2H_4.H_2O$) as a reducing agent and brown seaweed alginate as a stabilizing agent. The brown seaweed alginate was identified as the surfactant, which affects the particle size of Cu_2O@Cu nanomaterial. The formation of Cu_2O@Cu nanoparticles is easily discernible from the changes in the color of the solution. The color of the mixed solution changed immediately, shifting from a blue to a reddish-brown dispersion, suggesting the production of copper nanoparticles showed in figure 1

The XRD patterns of the brown seaweed alginate and alginate-stabilized Cu_2O@Cu nanoparticles were presented in figure 2.

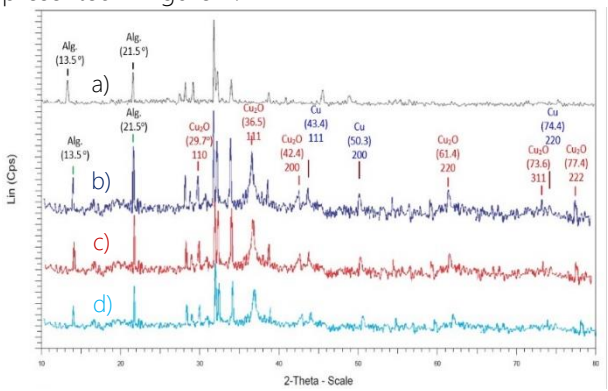

Figure 2: XRD patterns of the brown seaweed alginate (a) and alginate-stabilized Cu_2O@Cu nanoparticles with different alginate concentrations: 4% (b), 5% (c), 6% (d)

Figure 2a showed that the extracted alginate from the brown seaweed displayed two characteristic peaks at 2θ of 13.5° and 21.5° [14]. There were also peaks at 2θ of 28.2°, 44.0°, 50.1°, and 78.1°, which validated the crystalline form of alginate with organic and inorganic impurities in the brown seaweed. Fig. 2b, 2c, and 2d showed the XRD patterns of alginate-stabilized Cu_2O@Cu nanoparticles samples with various alginate concentrations, namely 4%, 5%, and 6%. The diffraction patterns displayed the distinctive peaks of two phases including crystalline metallic copper (cubic) and Cu_2O (cubic), implying that Cu^{2+} ions were chemically reduced to Cu and Cu^{+}. The XRD patterns of Cu_2O showed six peaks at 29.7°, 36.5°, 42.4°, 61.4°, 73.6°, and 77.4° matching properly with (110), (111), (200), (220), (311), and (222) planes of the face-centered cubic (fcc) structure, which is in a good agreement with the Cu_2O powder peaks obtained from of the International Centre of Diffraction Data card (JCPDS file no. 34-1354) [15]. The XRD patterns also display the peaks for Cu at 2θ of 43.4° (111), 50.6° (200), and 74.3° (220). All peaks areattributed to the cubic form of metallic copper [15-17], which is remarkably close to those provided by JCPDS file no. 04-0836 of XRD for Cu. These results are also following research of Badawy et al. and Maximino et al [18,19].

FT-IR spectra of brown seaweed alginate and alginate-stabilized Cu_2O@Cu nanoparticles with various alginate concentrations (4%, 5%, and 6% wt) of were shown in figure 3.

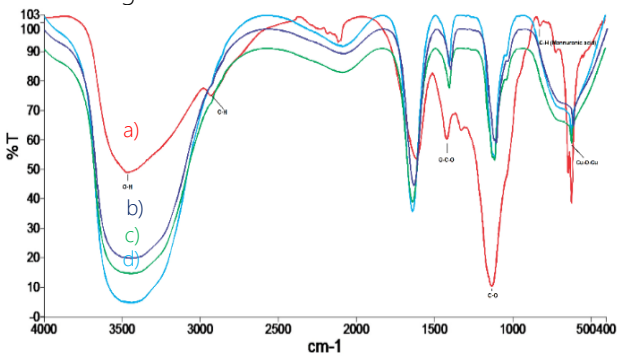

Figure 3: FT-IR spectra of the brown seaweed alginate (a) and alginate-stabilized Cu_2O@Cu nanoparticles with different alginate concentrations: 4% (b), 5% (c), 6% (d)

Figure 3a showed the stretches corresponding to mannuronic acid, OH, and CH_2 functional groups at 831 cm^{-1}, 3472 cm^{-1}, and 2926 cm^{-1}, respectively. Two strong absorptions were observed at 1610 cm^{-1} and 1415 cm^{-1} which were attributed to the asymmetric and symmetric stretching vibrations of carboxylate groups (O-C-O) [16]. The band at 1122 cm^{-1} was assigned to C-O stretching of pyranose. The comparison between FT-IR spectra of alginate (figure 3a) and alginate-stabilized Cu_2O@Cu nanoparticles (figure 3b, 3c, 3d) showed a blueshift of the absorption peak from 3462 cm^{-1} to 3430 cm^{-1} and decrease in intensity of the absorption at 2926 cm^{-1} due to the interaction of Cu^0 with -OH groups [17]. When stabilization occurred, the band corresponding to -C-O- stretching showed bathochromic shift from 1128 cm^{-1} to 1109 cm^{-1} [19]. Furthermore, the characteristic bands in the range of 618-637 cm^{-1} were ascribed to the vibrational mode of Cu-O in the Cu_2O phase [16,17], thereby confirming the formation of Cu_2O nanoparticles.

The UV-Vis absorption spectra of the alginate-Cu^{2+} complex and alginate-stabilized Cu_2O@Cu nanoparticles were presented in fig. 4. In the UV-Vis spectra of nanomaterials, the presence of absorption band in the range of 550-600 nm belonging to metallic Cu nanoparticles and the absence of absorption band in the range of 300-500 nm corresponding to Cu_2O nanoparticles reveal the formation of Cu_2O@Cu core-

https://doi.org/10.51316/jca.2021.098

shell nanoparticles [16]. The absorption peak at 234 nm is assigned to alginate-Cu^{2+} complex.

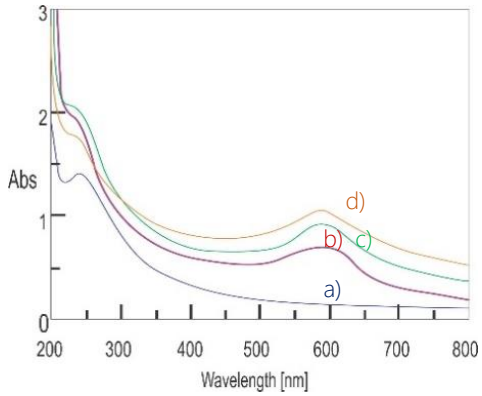

Figure 4: UV-Vis spectra of sodium alginate-Cu^{2+} complex (a) and alginate-stabilized Cu_2O@Cu nanoparticles with different alginate concentrations: 4% (b), 5% (c) and 6% (d)

The formation of the Cu shell could be explained as follows. As N_2H_4 was added into the system, in which the molar ratio of $CuSO_4/N_2H_4$ ~ 4/1, the Cu^{2+} ions were firstly reduced to Cu^+ ions, and the Cu_2O@Cu_2O nanoparticles could be formed [20,21]. When the addition of N_2H_4 was kept continuing, Cu_2O nanoparticles were formed initially, and subsequently, Cu_2O were reduced further by hydrazine to transform to copper hierarchical nanostructures, which can be described by the following reaction: $2Cu_2O + N_2H_4 \rightarrow 4Cu + N_2\uparrow + 2H_2O$ [20,22]. Thus, the Cu_2O@Cu_2O core-shell nanoparticles would be converted to Cu_2O@Cu core-shell nanoparticles stabilized by alginate. The obtained results are similar to those of our previous study [12].

Effect of alginate concentration on the size of Cu_2O@Cu nanoparticles

TEM images and particle size distribution of alginate-stabilized Cu_2O@Cu nanoparticles obtained from experiments with alginate concentration from 4% - 6% are shown in figure 5. The results obviously showed that Cu_2O@Cu nanoparticle size decreased when concentration of the alginate stabilizer increased. In particular, the Cu_2O@Cu nanoparticle size was 8.7 ± 1.8 nm with alginate concentrationof 4%, decreased to 5.5 ± 1.6 nm with alginate concentration of 5% and to 3.7 ± 1.7 nm with alginate concentration of 6%. The Cu_2O@Cu nanoparticles are spherical, relatively uniform and distributed in a narrow range. It is known that surfactants or polymers cause decrease in particle size due to the spatial effect. They prevent particles from coming together to agglomerate into larger particles [13]. However, when the glue solution achieves the necessary flexibility, the surfactant polymer content cannot be too high because solutions with a large viscosity are difficult to apply. Therefore, the solution with 6% wt of alginate is too concentrated and difficult to use.

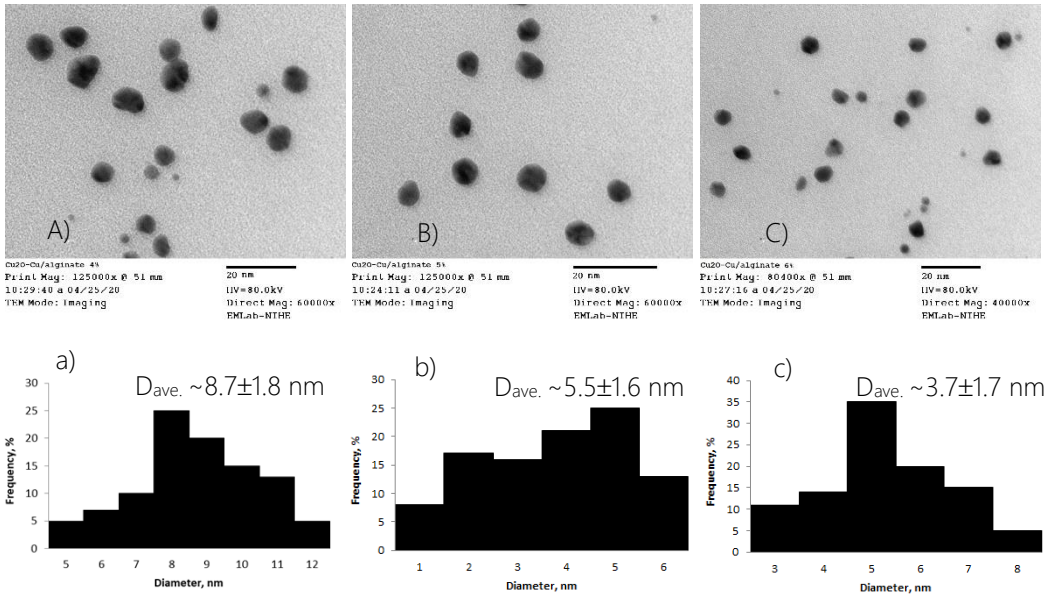

Figure 5: TEM images and particle size distributions of alginate-stabilized Cu_2O@Cu nanoparticles with different alginate concentration: 4% (A, a), 5% (B, b), 6% (C, c)

https://doi.org/10.51316/jca.2021.098

Conclusion

The alginate concentration affects the particle size of alginate-stabilized Cu_2O@Cu nanoparticles. The particle size is in the range of 3.7-8.7 nm corresponding to alginate concentration of 4-6% and decreased when the alginate concentration increased. The alginate-stabilized Cu_2O@Cu nanoparticles had a mixture crystal structure of Cu_2O and metallic Cu. The Cu_2O@Cu_2O core-shell structure would be converted to Cu_2O@Cu core-shell structure. With small particle size, the alginate-stabilized Cu_2O@Cu nanoparticle solution can be used as a fungicide to replace toxic agrochemicals and potentially applied to the development of sustainable agricultural production.

Acknowledgments.

This research was funded by the Program of Science and Technology for the Sustainable Development of the Mekong Delta Region under grant number KHCN-TNB.ĐT/14-19/C38.

References

1. T. Jay, G. C. Ratiram, V. G. Nilesh, R. R. Alok, Y. Sachin, D. J. Harjeet, J. Exp. Nanosci. 11(11) (2016) 884-900. https://doi.org/10.1080/17458080.2016.1177216
2. K. Giannousi, G. Sarafidis, S. Mourdikoudis, A. Pantazaki, C. Dendrinou-Samara, Inorg. Chem. 53(18) (2014) 9657-9666. https://doi.org/10.1021/ic501143z
3. K. P. Ajay, G. C. Ratiram, B. C. Prashant, Y. Sachin, M. Aniruddha, N. S. Vaishali, R. R. Alok, D. J. Harjeet, Mater. Sci. Eng. C 99 (2019) 783-793. https://doi.org/10.1016/j.msec.2019.02.010
4. B. D. Du, D. V. Phu, L. A. Quoc, N. Q. Hien, J. Nanopart. (2017) Article ID 7056864, 1. https://doi.org/10.1155/2017/7056864
5. Regmi, J. Bhandari, S. Bhattarai, S. K. Gautam, J. Nep. Chem. Soc. 40 (2019) 5-10. https://doi.org/10.3126/jncs.v40i0.27271
6. Eivazihollagh, M. Norgren, C. Dahlström, H. Edlund, Nanomater. 8 (2018) 238 (11pp). https://10.3390/nano8040238
7. N. Gu, J. Gao, H. Li, Y. Wu, Y. Ma, K. Wang., Appl. Clay Sci. 79 (2016) 132-133. https://doi.org/10.1016/j.clay.2016.05.017
8. S. Pandey, J. Ramontja, Int. J. Biol. Macromol. 93 (2016) 712-723. https://doi.org/10.1016/j.ijbiomac.2016.09.033
9. R. G. Chikte, K. M. Paknikar, Jyutika M. Rajwade, J. Sharma, Appl. Microbiol. Biotechnol. 103(11) (2019) 4605. https://doi.org/10.1007/s00253-019-09740-z
10. S. Huang, L. Wang, L. Liu, Y.Hou, and L. Li, Agron. Sustain. Dev. 35(2) (2015) 369–400. https://doi.org/10.1007/s13593-014-0274-x
11. D. Du, D. T. B. Ngoc, N. D. Thang, L. N. A. Tuan, B. D. Thach, N. Q. Hien, Vietnam J. Chem. 57(3) (2019) 318. https://doi.org/10.1002/vjch.201900022
12. T. B. Ngoc, B. D. Du, L. N. A. Tuan, B. D. Thach, T. P. Tho, D. V. Phu, Adv. Nat. Sci.: Nanosci. Nanotechnol., 2021, 12, 013001. https://iopscience.iop.org/article/10.1088/2043-6262/abebd6/meta
13. T. B. Ngoc, B. D. Du, L. N. A. Tuan, B. D. Thach, C. T. Kien, D. V. Phu, N. Q. Hien, Indian J. Agric. Res. 54(6) (2020) 802-806. https://10.18805/IJARe.A-582
14. R. A. Khajouei, J. Keramat, N.R Hamdami, A.-V. Ursu, C. Delattre, C. Laroche, C. Gardarin, D. Lecerf, J. Desbrières, G. Djelveh, P. Michaud, Inter. J. Biol. Macromol. 118 (2018) 1073-1081. https://10.1016/j.ijbiomac.2018.06.154
15. S. S. Sawant, A. D. Bhagwat, C. M. Mahajan, J. Nano Elec. Phys. 8(1), (2016) 01035 (5pp). https://10.21272/jnep.8(1).01036
16. H. Khanehzaei, M. B. Ahmad, K. Shameli, Z. Ajdari., Int. J. Electrochem. Sci. 9 (2014) 8189-8198. http://www.electrochemsci.org/papers/vol9/91208189.pdf
17. J. Diaz-Visurraga, C. Daza, C. Pozo, A. Becerra, C. V. Plessing, A. Garcia, Int. J. Nanomedicine 7 (2012) 3597-3612. https://10.2147/IJN.S32648
18. S. M. Badawy, R. A. El-Khashab, A. A. Nayl, Bull. Chem. React. Eng. Catal. 10(2) (2015) 169-174. https://doi.org/10.9767/bcrec.10.2.7984.169-174
19. N. J. Maximino, M. P. Alvarez, R. S. Avila, C. A. Orta, E. J. Regalado, J. Nanomater. (2018) Article ID 9512768 1. https://doi.org/10.1155/2018/9512768
20. L. Yang, S. P. Li, Y. J. Wang, L. L. Wang, X. C. Bao, R. Q. Yang, Trans. Nonferrous Met. Soc. China. 25 (2015) 3643-3650. https://doi.org/10.1016/S1003-6326(15)64005-5

21. M. Behera, G. Giri, Mater. Sci.-Poland 32(4) (2014) 702-708. https://doi.org/10.2478/s13536-014-0255-4

22. V. Andal, G. Buvaneswari, Eng. Sci. Technol. Int. J. 20 (2017) 340-344. https://doi.org/10.1016/j.jestch.2016.09.003